



Multicomponent seismic data conditioning and joint PP-PS inversion

Anderson W. P. de Franco* (LENEP/UENF, Brazil), Fernando S. de Moraes (LENEP/UENF, Brazil) and Carlos E. Theodoro (PETROBRAS, Brazil)

Copyright 2015, SBGf - Sociedade Brasileira de Geofísica

This paper was prepared for presentation during the 14th International Congress of the Brazilian Geophysical Society held in Rio de Janeiro, Brazil, August 3-6, 2015.

Contents of this paper were reviewed by the Technical Committee of the 14th International Congress of the Brazilian Geophysical Society and do not necessarily represent any position of the SBGf, its officers or members. Electronic reproduction or storage of any part of this paper for commercial purposes without the written consent of the Brazilian Geophysical Society is prohibited.

Abstract

Joint interpretation and inversion of multicomponent PP and PS can be a difficult task to perform in a consistent way. This difficulty arises because PP and PS records are different in essential aspects, including seismic event time registration, frequency content and earth reflectivity. In this work, we develop seismic data conditioning workflows for both PP and PS data, with the objective of performing a joint PP-PS AVO inversion. This study focuses on PP and PS pre-stack data conditioning for multicomponent simultaneous joint inversion.

Introduction

Joint AVO inversion of multicomponent data is a useful technique to estimate elastic properties, and can be used to characterize reservoirs, once they are related to lithology, texture, rock structure and fluid content. Inverting both PP and PS data makes density estimation more reliable (Niebuda et. al., 2008) than the conventional AVO inversion of PP data alone. As converted wave reflectivity depends mainly on VS (shear wave velocity) and density, it provides an additional source of information with respect to conventional PP data dominated by near offset response or P-impedance.

This technique consists in the simultaneous inversion of two volumes PP and PS, resulting in parameters, such as P-impedance and S-impedance, together in the same inversion. The application of joint inversion allows improvement in the results of converted wave, usually resulting in better resolution of S-impedance and even better resolution of density, with good conditions of signal-to-noise ratio, when compared to PP-inversion (Larsen, 1999). Joint AVO inversion has been widely studied, as by Mahmoudian & Margrave (2003), Hampson et al. (2005) and Deng et al. (2011).

The data conditioning is one of the most important steps of the inversion. Besides all the treatment realized to improve the signal-to-noise ratio, it's important to declare the necessity of the preservation of amplitudes so the result of the inversion don't be compromised. Thus, a quality control should be performed in each stage for the preservation of signal. As well as amplitude preservation, the conciliation of PS and PP time is very important before the application of joint inversion.

Theory and Method

The approach used in the Zoeppritz equation for joint AVO inversion PP-PS was Aki-Richards (2002), where is obtained the estimates of R_P (p-wave reflectivity), R_S (s-wave reflectivity), and R_D (density reflectivity)

The equation of reflectivity PP ($R_{PP}(\theta)$) rewritten in terms of impedance reflectivity R_P , R_S e R_D as given by:

$$R_{PP}(\theta) = C_1 R_P + C_2 R_S + C_3 R_D, \quad (1)$$

where

$$C_1 = 1 + \tan^2 \theta, \quad (2)$$

$$C_2 = -8\gamma^2 \sin^2 \theta, \quad (3)$$

$$C_3 = -\frac{1}{2} \tan^2 \theta + 2\gamma^2 + \sin^2 \theta, \quad (4)$$

$$\gamma = \frac{V_S}{V_P}, \quad (5)$$

$$R_P = \frac{1}{2} \left[\frac{\Delta V_P}{V_P} + \frac{\Delta \rho}{\rho} \right], \quad (6)$$

$$R_S = \frac{1}{2} \left[\frac{\Delta V_S}{V_S} + \frac{\Delta \rho}{\rho} \right], \quad (7)$$

and

$$R_D = \frac{\Delta \rho}{\rho}. \quad (8)$$

In above equations, V_P and V_S are P and S-wave velocities, respectively, and θ is the angle of incidence V_P . Considering the relationship between the properties of two layers defined as 1 and 2:

$$\Delta V_P = V_{P2} - V_{P1}, \quad (9)$$

$$\Delta V_S = V_{S2} - V_{S1}, \quad (10)$$

$$\Delta \rho = \rho_2 - \rho_1, \quad (11)$$

$$V_P = \frac{V_{P2} + V_{P1}}{2}, \quad (12)$$

$$V_S = \frac{V_{S2} + V_{S1}}{2}, \quad (13)$$

and

$$\rho = \frac{\rho_2 + \rho_1}{2}. \quad (14)$$

The equation of PS reflectivity from the Aki & Richards (2002) rewritten in terms of impedance reflectivity R_S and R_D (Larsen, 1999) is written as

$$R_{PS}(\theta, \varphi) = C_4 R_S + C_5 R_D, \quad (15)$$

where

$$C_4 = \frac{4 \tan \varphi}{\gamma} (\sin^2 \varphi - \gamma \cos \theta \cos \varphi), \quad (16)$$

$$C_5 = \frac{-\tan \varphi}{2\gamma} (1 + 2 \sin^2 \varphi - 2\gamma \cos \theta \cos \varphi), \quad (17)$$

and

$$\varphi = \sin^{-1}(\gamma \sin \theta), \quad (18)$$

being φ the angle of reflection Vs.

One of the simplest ways to implement the AVO inversion is done by taking the AVO curves in each same time of the image gather. In that case we may consider the geometry of each seismogram to be inverted, as being composed of a set of N samples at each time spaced relative to the center of cell migration is represented by h_i , $i = 1, \dots, N$. In this case, the AVO curve can be written in matrix notation as given by:

$$\mathbf{d}^{\text{calc}} = \mathbf{Gm} \quad (19)$$

The data is modeled by a linear function of AVO equations (1) and (15), described by the matrix:

$$\begin{bmatrix} R_{PP}(\theta_1) \\ \vdots \\ R_{PP}(\theta_N) \\ R_{PS}(\theta_1, \varphi_1) \\ \vdots \\ R_{PS}(\theta_N, \varphi_N) \end{bmatrix} = \begin{bmatrix} C_1(\theta_1) & C_2(\theta_1) & C_3(\theta_1) \\ \vdots & \vdots & \vdots \\ C_1(\theta_N) & C_2(\theta_N) & C_3(\theta_N) \\ 0 & C_4(\theta_1, \varphi_1) & C_5(\theta_1, \varphi_1) \\ \vdots & \vdots & \vdots \\ 0 & C_4(\theta_N, \varphi_N) & C_5(\theta_N, \varphi_N) \end{bmatrix} \begin{bmatrix} R_P \\ R_S \\ R_D \end{bmatrix}. \quad (20)$$

In the context of Bayesian inference, the problem is to determine the posteriori probability density for the parameter vector \mathbf{m} from a set of noisy observations $\mathbf{d}^{\text{obs}} \in \mathfrak{R}^N$, which can be written as:

$$\mathbf{d}^{\text{obs}} = \mathbf{Gm} + \mathbf{n}, \quad (21)$$

where $\mathbf{n} \in \mathfrak{R}^N$ is the noise contained in data. In this case, the formulation for obtaining the posterior distribution is given by:

$$p(\mathbf{m} | \mathbf{d}^{\text{obs}}) = k q(\mathbf{m}) r(\mathbf{d}^{\text{obs}} | \mathbf{m}), \quad (22)$$

where k is a normalization constant, q and r are the priori distribution and the likelihood function, respectively, for the parameters. From the posterior distribution estimates $\hat{\mathbf{m}}$ and associated measures of uncertainty, such as mean and covariance are obtained.

Likelihood function r

We can explain the formulation of the problem of Bayesian inference, by defining probability models, starting with the likelihood function. The likelihood function is constructed based on the uncertainty of the data, or based on the noise, as defined in equation (21). Whereas moments of the first and second order will be enough to describe the errors contained in the data, the proper choice is the normal distribution $\mathbf{d} | \mathbf{m} \sim N(\mathbf{Gm}, \sigma^2 \mathbf{I})$, which can be represented by

$$r(\mathbf{d} | \mathbf{m}, \sigma^2) = (2\pi\sigma^2)^{-\frac{N}{2}} \exp\left[-\frac{1}{2\sigma^2} (\mathbf{d} - \mathbf{Gm})^T (\mathbf{d} - \mathbf{Gm})\right], \quad (23)$$

where σ^2 is the data variance. Typically, the variance of the data is unknown, making it an additional parameter to be estimated, in trouble, or marginalized as standard solution adopted in Bayesian inference (see for example, Box and Tiao, 1973). With the introduction of this extra parameter, it becomes necessary to revise the final shape of the posterior distribution (equation 22) as given by:

$$p(\mathbf{m}, \sigma^2 | \mathbf{d}^{\text{obs}}) = k w(\sigma^2) q(\mathbf{m}) r(\mathbf{d}^{\text{obs}} | \mathbf{m}, \sigma^2), \quad (24)$$

Being w the prior distribution for the variance of the data.

Priori Distribution q

In the case of the priori distribution, we can adopt a conservative approach and consider little information distributions, which were listed for the attributes of reflectivity R_P and R_S , and uninformative distribution of Jeffreys for the variance of the data, implying that:

$$q(\mathbf{m}) \propto c, \quad (25)$$

and

$$w(\sigma^2) \propto \frac{1}{\sigma}, \quad \text{for } 0 \leq \sigma \leq \infty. \quad (26)$$

Posteriori Distribution p

Following equation (24) and combining equations (23), (25) and (26) we obtain the general expression for the joint posteriori distribution and variance parameters for the subsequent data, as given by:

$$p(\mathbf{m}, \sigma^2 | \mathbf{d}^{\text{obs}}) \propto \frac{1}{\sigma^{N+1}} \exp\left[-\frac{1}{2\sigma^2} (\mathbf{d} - \mathbf{Gm})^T (\mathbf{d} - \mathbf{Gm})\right]. \quad (27)$$

Note that the main interest is to infer on the parameters \mathbf{m} consisting of the attributes of reflectivity, without interest

in estimating the variance of data. In this case, the standard procedure of the Bayesian inference is to eliminate this type of variable through integration which can be represented by:

$$p(\mathbf{m} | \mathbf{d}^{\text{obs}}) = \int_0^{\infty} p(\mathbf{m}, \sigma^2 | \mathbf{d}^{\text{obs}}) d\sigma. \quad (28)$$

The result of this integration is the marginal posterior distribution, which now depend only on the parameters of interest. In this case, the final shape of the posterior distribution can be written as:

$$p(\mathbf{m} | \mathbf{d}^{\text{obs}}) \propto \frac{1}{\left[(\mathbf{d} - \mathbf{G}\mathbf{m})^T (\mathbf{d} - \mathbf{G}\mathbf{m}) \right]^{\frac{N_i}{2}}}. \quad (29)$$

Conditioning

In this work, we develop a seismic data conditioning workflow for both PP and PS data, aiming the performing the joint PP-PS AVO inversion.

In order to conditioning PP and PS unstacked, distinct fluxes were created due to different types of noises found in each data. Along each step of the process quality control has been made to preserve the amplitudes, and so guarantee a reliable inversion. The PP and PS data conditioning steps can be seen in the flows of Figure 1.

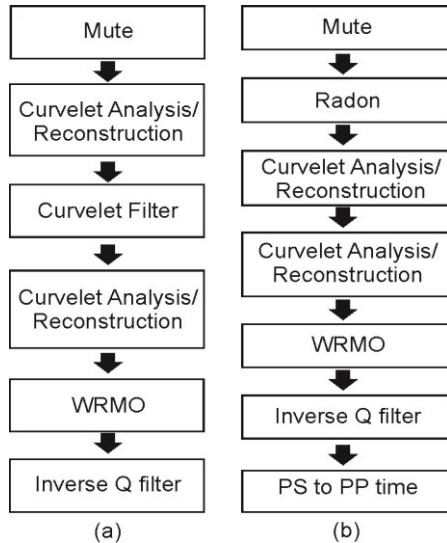


Figure 1: (a) PP conditioning flow and (b) PS conditioning flow.

In PP data conditioning, the first step was the application of the mute in order to remove noises above the reflector of the sea floor and to remove traces that suffered stretch. Then, it was applied Curvelet Analysis/Reconstruction (Braga, 2011) to remove coherent noise and multiples. After this step it was applied the Curvelet filter (Braga, 2011) to remove random noises. After improvement of the signal-to-noise ratio other coherent noises were observed, showing the necessity of the application of Curvelet Analysis/Reconstruction once more with different parameters. Better signal-to-noise it was applied a WRMO (wavelet based residual move out) tool (Braga,

2011) to correction residual normal move out of the events from the Wavelet transform. In the final stage it was applied the Inverse Q Filter (Braga, 2013) to correct the attenuation effect.

In PS data conditioning, it was applied the mute to achieve the removal of noises above the reflector of the sea floor and of the traces that suffered stretch. Then the Radon transform was applied for removing multiples. After the application of Curvelet filter coherent noises were observed, which were removed by Curvelet Analysis/Reconstruction. In the next step, it was realized the conversion of PS time to PP time, which allows the correlation between PS and PP data. After achievement of a better signal-to-noise, it was applied a WRMO tool to correct residual normal move out. In the final stage, it was applied the inverse Q filter in order to correct the attenuation effect.

Synthetic data were created from the well logs and used as a parameter to compare each step of PP data with AVO curves generated for comparison between original, conditioned and synthetic data (Figure 2 and Figure 3). The same was done for PS data (Figure 4 and Figure 5).

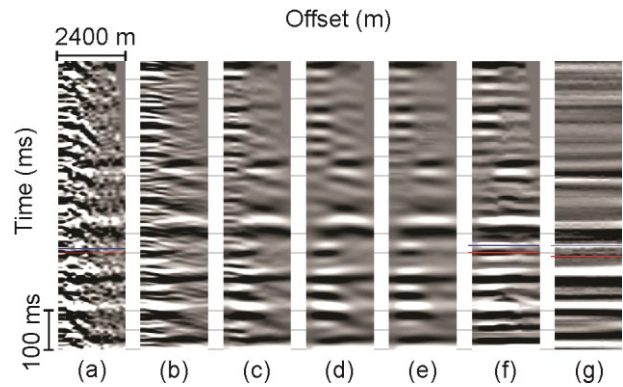


Figure 2: Stages of conditioning as PP, being compared to the synthetic data. (a) Section after original mute, (b) Curvelet Analysis / Reconstruction (c) Curvelet filter, (d) Curvelet Analysis/Reconstruction, (e) residual move out correction (WRMO), (f) Application of inverse Q filter, (g) synthetic data. In blue and red are represented the negative and positive reflectors for AVO analysis.

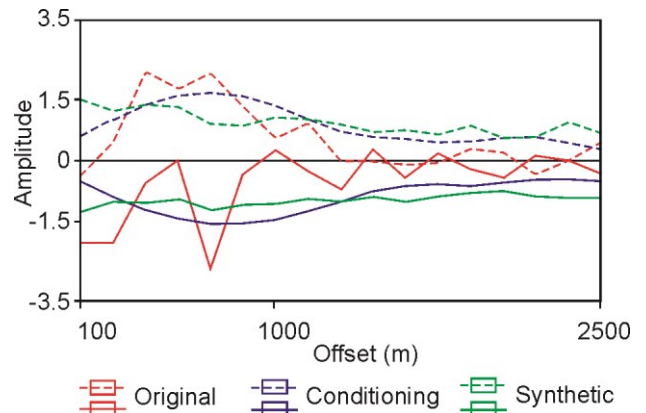


Figure 3: AVO curves for the given PP. The curves shown in red correspond to the original data migrated, green to the data conditioned PP and in blue to the synthetic data.

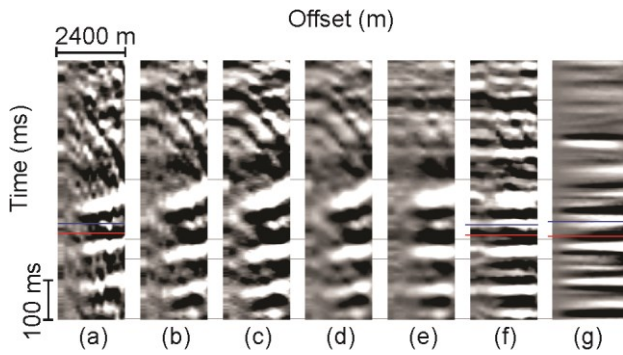


Figure 4: Stages of conditioning as PS, being compared to the synthetic data. (a) Section after original mute, (b) Radon Transform (c) Curvelet Analysis / Reconstruction (d) Curvelet Filtering, (e) residual move out correction (WRMO), (f) Application of inverse Q filter, (g) synthetic data. In blue and red are represented the negative and positive reflectors for AVO analysis.

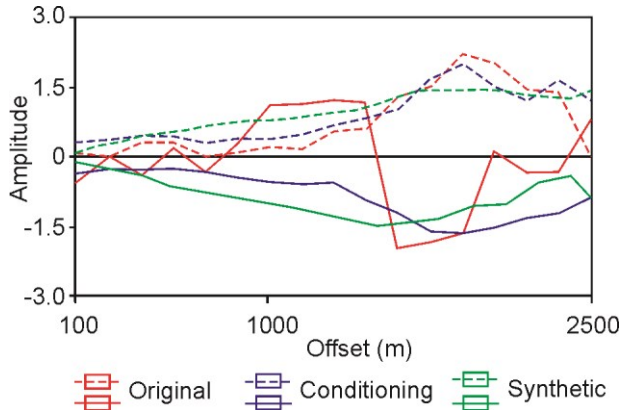


Figure 5: AVO curves for the given PS. The curves shown in red correspond to the original data migrated, green to the data conditioned PS and in blue to the synthetic data.

In the Figure 6, PP and PS seismic stacked sections of original and conditioned data are presented. In these sessions can be noticed the significant improvement in resolution of data after conditioning, as well as the PP and PS spectra equalization when compared to the originals presented in Figure 7.

In Figure 8 it's possible to compare between the elastic parameters curves from original data and conditioned data with those from the well.

Background models were created for P-impedance, S-impedance and density to obtain the absolute impedances and density. These models were obtained from the construction of horizons and the use of well logs after applying a low pass filter with a maximum frequency of 8 Hz.

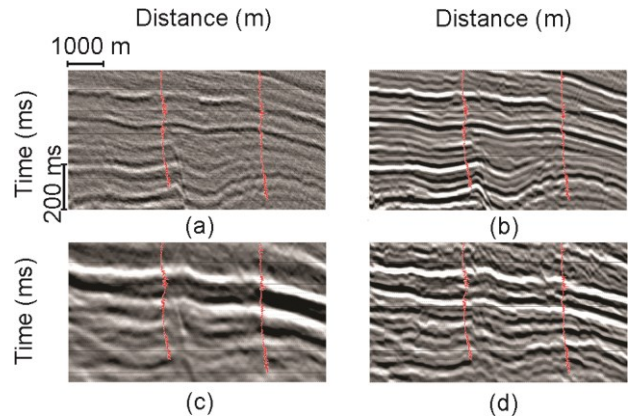


Figure 6: (a) PP original stacked section, (b) PP conditioned section. (c) PS original stacked section and (d) PS conditioned section.

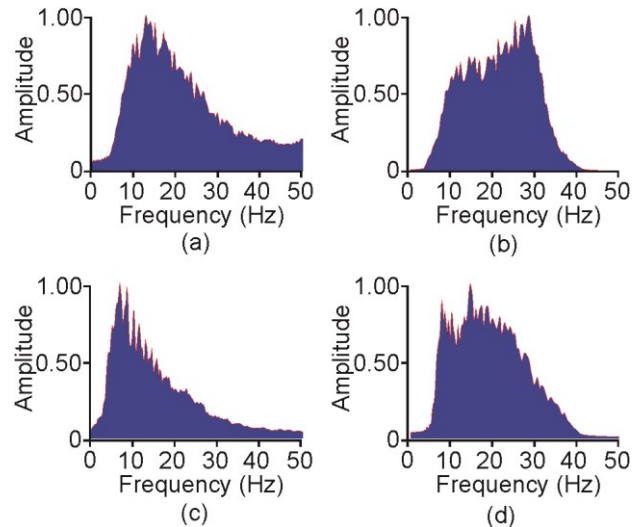


Figure 7: frequency spectrum of (a) the original PP data, (b) conditioned PP data, (c) original PS data and (d) of the conditioned PS data.

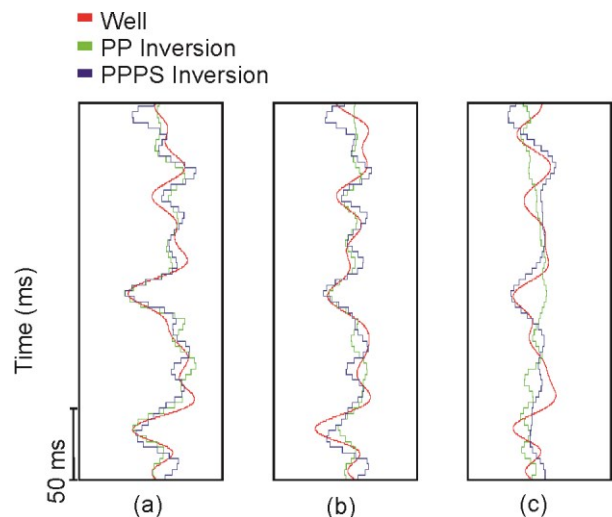


Figure 8: well logs in red, original data in green and conditioned data in blue (a) variation curves of the P-impedance; (b) variation curves of the S-impedance (c) variation curves of density.

Finally, the absolute P-impedance, S-impedance and density obtained, represented in Figure 9. These absolute values were obtained by summing across the background, for recompose the lost by the low frequency seismic data.

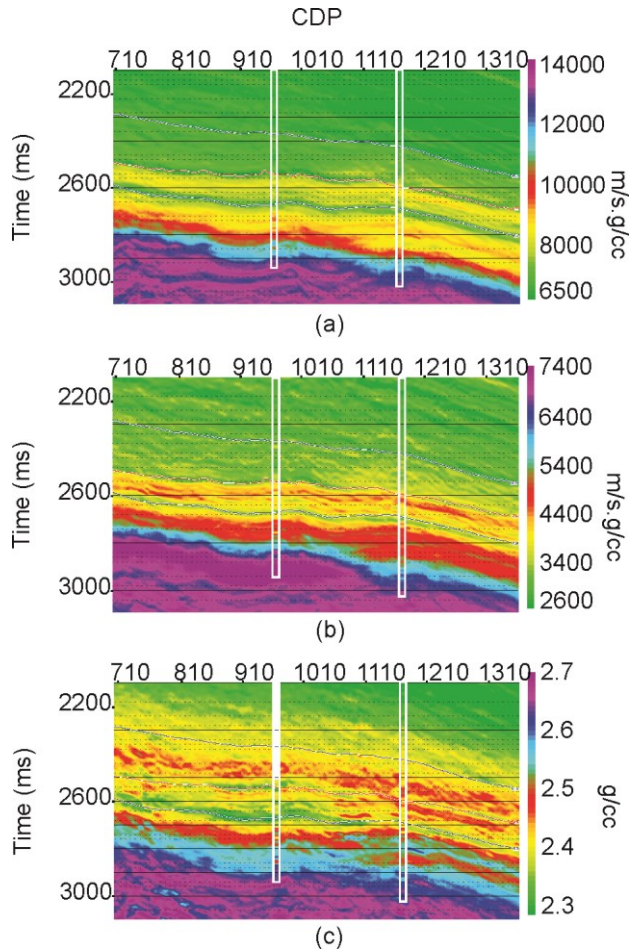


Figure 9: The sections represent the elastic parameters derived from joint PP-PS inversion compared to wells (outlined in white). The parameters are represented respectively: (a) P-impedance (a), (b) S-impedance and (c) Density.

Conclusions

In the end of PP and PS data conditioning, it was possible to notice significant improvement in the signal-to-noise ratio and the registration of PP and PS events. Comparing the inversion results of original data and conditioned data, it's noticed that conditioned data presents an improvement in S-impedance and a significant improvement in density when collated to well data.

Acknowledgments

We thank the entire group GIR (LENEP/ UENF) and the teacher Sergio Oliveira. We also thank Igor Braga and INVISION by the use of some tools used in this work and PETROBRAS for the support.

References

- Aki, K., and P. G. Richards, 2002, Quantitative Seismology, 2nd edn. University Science Books, Sausalito, CA.
- Box, G. E. P., and G. C. Tiao, 1973, Bayesian inference in statistical analysis, Addison-Wesley, Reading, MA.
- Braga, I. L. S., 2011, Técnicas multiespectrais aplicada a fluxos de inversão e caracterização de reservatórios de hidrocarbonetos: Ph.D. thesis, Universidade Estadual Norte Fluminense, Brazil (in portuguese).
- Braga, I. L. S., and Moraes, 2013, High-resolution gathers by inverse Q Filtering in the wavelet domain: Geophysics, v. 78, no. 2, P.V53-V61.
- Deng, Z., Sen, M. K., Wang, U., Bai, X. and Xue, Y., 2011, Prestack PP & PS wave joint stochastic inversion in the same PP time scale: Ann. Mtg. Abstracts, SEG, p. 1303-1307.
- Hampson, D.P., Russell, B.H., and Bankhead, B., 2005, Simultaneous inversion of pre-stack seismic data: Ann. Mtg. Abstracts, SEG, p. 1633-1637.
- Larsen J.A., 1999, AVO inversion by simultaneous PP and PS inversion: M.Sc. Thesis, University of Calgary.
- Mahmoudian F. and Margrave, G.F., 2003, AVO inversion of multicomponent data for P and S impedance: CREWES Research Report, Vol. 15, p. 1-34.
- Niebuda M., Mesdag P. and Daniels J., 2008, Oseberg South PP-PS Joint (AVA) inversion. Fugro-Jason AS and StatoilHydro ASA, Norway.